



ARTICLE

Graphite-Rich Phyllonitic Metapelites and Metamafic Rocks from the Itatiaiuçu Region of Southern Sao Francisco Craton: Remnants of Paleoproterozoic Forearc Basin

Raphael Martins Coelho ^{1*} , Alexandre de Oliveira Chaves ¹ , Roberto Moreno Prado Pereira ¹ , Carla Cristine Porcher ² 

¹ Institute of Geosciences, Federal University of Minas Gerais, Belo Horizonte 31270-901, Brazil

² Institute of Geosciences, Federal University of Rio Grande do Sul, Porto Alegre 90650-001, Brazil

ABSTRACT

The area in the southern São Francisco Craton, between Itatiaiuçu and Rio Manso (Minas Gerais), constitutes a geological domain that remains poorly constrained regarding the nature, age, and tectono-metamorphic evolution of its metamafic and metasedimentary units. A marked contrast in gamma-spectrometric signatures—expressed by darker tones relative to the surrounding Archean terranes—delineates a distinct lithological association composed of tremolite–actinolite schists, metaconglomerates with strongly stretched clasts, and phyllonitic metapelites containing quartz, graphite ($\delta^{13}\text{C}$ values between -26‰ and -14‰ , consistent with an organic source), plagioclase, chlorite, phengite, amphibole, and garnet. The tremolite–actinolite schists yield paleoproterozoic Sm–Nd model ages between 2,354 and 2,110 Ma and positive ϵNd values (+0.56 to +3.53), indicating derivation from a mantle source. Mineral assemblages in the phyllonitic metapelites are compatible with metamorphism of a flysch-molasse-type mélange developed in a forearc basin associated with subduction-related shear processes within an accretionary orogen. In this framework, the tremolite–actinolite schists are interpreted as metamorphosed oceanic crust, representing remnants of an oceanic domain that separated the Campo Belo–Bonfim and Belo Horizonte

*CORRESPONDING AUTHOR:

Raphael Martins Coelho, Institute of Geosciences, Federal University of Minas Gerais, Belo Horizonte 31270-901, Brazil;
Email: raphaelmcoelho@yahoo.com.br

ARTICLE INFO

Received: 29 December 2025 | Revised: 27 February 2026 | Accepted: 12 March 2026 | Published Online: 27 March 2026
DOI: <https://doi.org/10.36956/eps.v5i1.3040>

CITATION

Coelho, R.M., de Oliveira Chaves, A., Pereira, R.M.P., et al., 2026. Graphite-Rich Phyllonitic Metapelites and Metamafic Rocks from the Itatiaiuçu Region of Southern Sao Francisco Craton: Remnants of Paleoproterozoic Forearc Basin. *Earth and Planetary Science*. 5(1): 62–74.
DOI: <https://doi.org/10.36956/eps.v5i1.3040>

COPYRIGHT

Copyright © 2026 by the author(s). Published by Nan Yang Academy of Sciences Pte. Ltd. This is an open access article under the Creative Commons Attribution-NonCommercial 4.0 International (CC BY-NC 4.0) License (<https://creativecommons.org/licenses/by-nc/4.0/>).

blocks around 2.3 Ga. The transition from oceanic to forearc basin conditions was accompanied by deformation within a thrust belt, where flysch and molasse sequences were metamorphosed to produce phyllonitic metapelites and metaconglomerates. Collectively, this domain preserves significant evidence of Paleoproterozoic geodynamic processes comparable to those observed in modern convergent plate settings.

Keywords: Itatiaiuçu; Tremolite-Actinolite Schists and Phyllonitic Metapelites; Flysch-Molasse-Type Mélange; Fore-arc Basin; Paleoproterozoic

1. Introduction

Accretionary orogens are characterized by the presence of accretionary complexes that incorporate mid-ocean ridge basalt (MORB) and deep-marine sediments derived from the subducting oceanic plate. These complexes are also associated with medium- to high-grade metamorphic rocks and calc-alkaline I-type batholiths belonging to the overriding continental plate. These domains are typically separated by a forearc basin^[1,2]. The closure of the oceanic basin is marked by a collisional suture zone that preserves remnants of oceanic lithosphere and related components^[3-6]. Several studies on modern orogens suggest that the mineral assemblage composed of quartz, graphite, plagioclase, chlorite, phengite, rutile, amphibole, and garnet is related to metamorphic conditions compatible with melanges formed in forearc basins during subduction events^[7-11].

The region located in the Southern São Francisco Craton, between Itatiaiuçu and Rio Manso (MG), constitutes a geological sector that is still poorly understood regarding the nature, age, and tectono-metamorphic evolution of its metamafic and metasedimentary rocks. Paleoproterozoic subduction events have already been described in neighboring areas, such as Itaguara^[12,13]. Therefore, there is a possibility that adjacent regions may still contain remnants of this process. The study area was delimited in the region between the cities of Itatiaiuçu and Rio Manso, where it is possible to observe a quite evident contrast represented by the dark tones in the gamma-spectrometric chart (ternary composition K-Th-U-CPRM-CODEMIG **Figure 1**) compared to the lighter tones of the Archean terrains around it. Within the study area, metamafic rocks and graphitic metapelitic rocks are strongly mylonitized (**Figure 2a**), and metaconglomerates with extremely elongated pebbles (**Figure 2b**) occur near a stream.

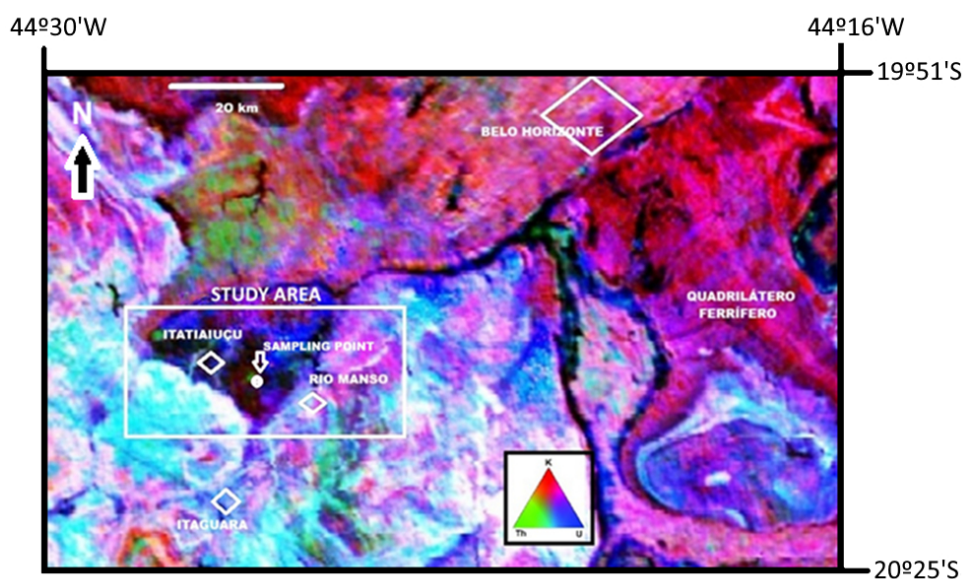


Figure 1. Gamaespectrometric Chart (Ternary Composition K-Th-U-CPRM-CODEMIG^[14]), with the Study Area and Sampling Point Locations.



Figure 2. (a) Metamafic rocks (left) and graphitic metapelitic rocks (right); (b) Metaconglomerate with stretched pebbles highlighted by the black arrows.

Source: All images are from a small stream between Rio Manso-MG and Itatiaiuçu-MG (Brazil).

The aim of this work is to characterize the metapelitic and metamafic rocks from the Itatiaiuçu region in terms of their petrology and ages to investigate their nature and tectono-metamorphic setting and their relationship with the flysch-molasse-type melange of a forearc basin in the context of a paleoproterozoic subduction event.

2. Geological Setting

The southern São Francisco Craton (SFC, **Figure 3b**) comprises essentially Archean granite-gneiss terranes and associated greenstone belts of the Rio das Velhas Supergroup, which includes mafic-ultramafic successions, intermediate to felsic volcanic units, volcanoclastic rocks, and clastic sediments^[15,16]. Overlying these sequences, the Paleoproterozoic Minas Supergroup consists of continental to marine (passive margin) metasedimentary rocks and banded iron formations of the Quadrilátero Ferrífero^[17,18]. The Archean crystalline basement is subdivided into the Divinópolis, Campo Belo/Bonfim, and Belo Horizonte complexes^[19] (**Figure 3a**), formed predominantly by TTG granitoids, gneisses, migmatites, and subordinate mafic-ultramafic lithotypes. Four major magmatic episodes characterize the evolution of the Archean crust^[20–22]: (1) the Santa Bárbara event (3,220–3,200 Ma), responsible for initial TTG crust formation; (2) the Mesoarchean Rio das Velhas I (2,920–2,850 Ma), reflecting crustal growth

through TTG magmatism and accretion of greenstone units; (3) the Neoarchean Rio das Velhas II (2,800–2,760 Ma); and (4) the potassic Mamona event (2,750–2,680 Ma), which stabilized the southern portion of the craton. Detrital zircon studies from the Rio das Velhas basin support the development of magmatic arcs and convergent basins until ca. 2.7 Ga^[23].

During the Paleoproterozoic, the SFC participated in the Rhyacian–Orosirian orogenic cycle (formerly “Transamazonian”), now redefined as the Minas accretionary orogeny, which contributed substantially to continental crustal growth^[15]. This orogeny amalgamated juvenile arcs, intra-oceanic sequences, and microcontinents to form the Mineiro Belt^[24–26]. The boundary between Campo Belo/Bonfim Complex and Mineiro Belt is delineated by the Jeceaba–Bom Sucesso Lineament^[27].

Within this orogenic framework, the Cláudio Shear Zone (CSZ) constitutes a NE–SW crustal-scale suture^[28] that separates the Campo Belo/Bonfim and Divinópolis complexes^[29,30]. Paleoproterozoic reworking is evidenced by the Kinawa migmatite (2,048–2,034 Ma^[31,32], formed through partial melting of 2.7 Ga TTGs at granulite–amphibolite facies. High-grade khondalitic sequences in the Itapeçerica region record metamorphic peaks at ca. 2.09–2.01 Ga^[29,33,34], whereas the peraluminous Água Rasa metagranite (1,934 ± 74 Ma) formed by anatexis of pelitic rocks during late-collisional stages^[35].

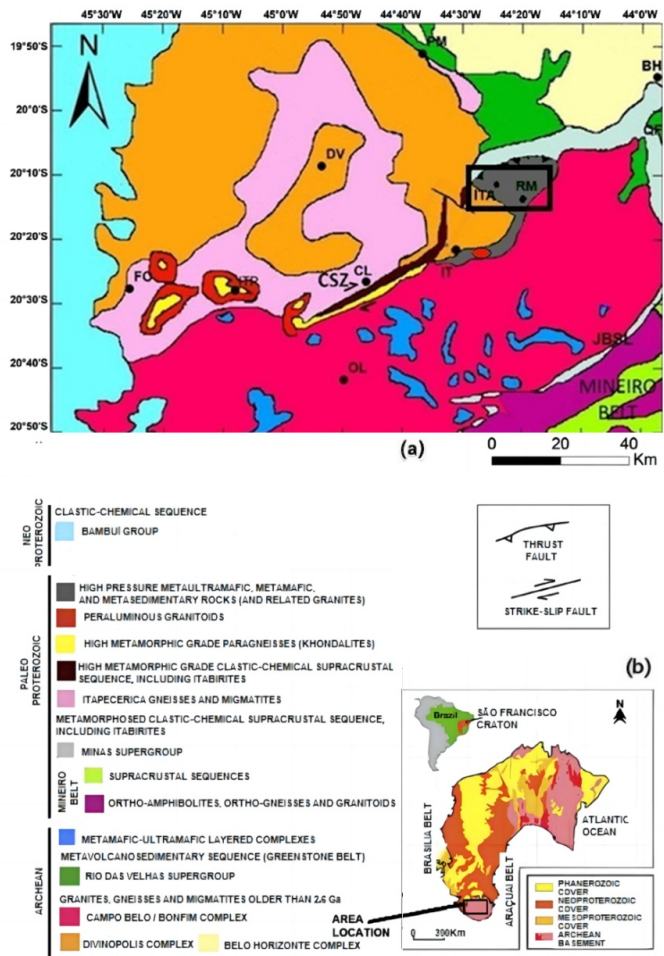


Figure 3. (a) Simplified geological map of the Southern São Francisco Craton; (b) The São Francisco Craton.

Note: QF—Quadrilátero Ferrífero, JBSL—Jeceaba-Bom Sucesso lineament, CSZ—Cláudio shear zone. Cities: BH—Belo Horizonte, PM—Pará de Minas, ITP—Itapeçerica, DV—Divinópolis, RM—Rio Manso, IT—Itaguara, FO—Formiga, CL—Cláudio, OL—Oliveira. ITA—Itatiaçu. The black polygon shows the studied area. Source: Modified from Chaves et al. [12].

The Itaguara Sequence (IS) consists of a tectonically reworked mafic-ultramafic layered complex derived from peridotitic and gabbroic protoliths. Garnet-bearing amphibolites yield crystallization ages of $2,159 \pm 21$ Ma and record metamorphic events between 2.06 and 2.03 Ga [36]. This sequence further comprises talc-actinolite metaultramafic rocks, banded iron formations, quartzites, mica-quartz schists, and the S-type Córrego do Peixoto granite, which formed through decompression melting during collisional processes at approximately 2.05 Ga [12]. Structurally, the IS delineates a narrow NE-SW-trending belt affected by dextral strike-slip and reverse fault systems [37].

Toward the northeast, the IS grades into the Rio Manso Sequence (RMS), which is predominantly composed of spinel-bearing metaultramafic lithologies inter-

preted as metamorphosed komatiitic assemblages [38,39]. Nevertheless, the presence of pseudo-spinifex olivine textures and high-grade mineral associations supports an ophiolitic affinity, representing fragments of oceanic lithosphere emplaced during Paleoproterozoic convergence [37]. The IS also preserves retroeclogites [13] and retro-blueschists [40] exhibiting E-MORB geochemical signatures, consistent with modern-style subduction operating between 2.20 and 2.13 Ga.

3. Methods

Five representative samples (three metapelites and two metamafic rocks) found in the study area (coordinates: 20.213893 S 44.375330 W) were selected for thin-section petrography and X-ray diffraction studies. The phyl-

lonites were also analyzed by Raman spectroscopy, and the graphite present in the samples was analyzed for carbon isotopes. The tremolite-actinolite schists were investigated using whole-rock Sm-Nd isotopic analyses to calculate depleted mantle model ages and epsilon Nd values.

3.1. Carbon Isotopes

Stable carbon isotope analyses were performed at the University of São Paulo (USP) CPGeo laboratory using a Delta V Advantage gas source isotope ratio mass spectrometer (IRMS) coupled to the Isolink Element Analyzer (Thermo). The tests were carried out by combustion at a temperature of 1,020 °C in the presence of O₂, using a quartz reactor packed with consumables specific for carbon isotope analysis ($\delta^{13}\text{C}$). The C results are expressed by δ , a conventional notation relative to the Vienna Pee-Dee Belemnite (VPDB) standard $\pm 2\text{SD}\%$ (95% confidence level).

3.2. Raman Spectroscopy

The Raman data were obtained in the Technological Center of Nanomaterials (CTNano) at the Technological Park of Belo Horizonte (MG)—BH Tec, using a confocal microscope Alpha300R WITEC (Wissenschaftliche Instrumente und Technologie GmbH®, Ulm, Germany) equipped with a Nd-YAG laser with double frequency (2.49 mW, $\lambda = 532.2$ nm). Raman spectra were collected with a 50 \times lens objective, where five scans in the 1,000–3,200 cm^{-1} spectra (first order = 1,000–2,000 cm^{-1} ; second order = 2,200–3,200 cm^{-1}) were performed with an acquisition time of 30 s.

3.3. X-Ray Diffraction (XRD)

The X-ray diffraction analyses (XRD) were performed at the Manoel Teixeira da Costa Research Center (CPMTC-IGC-UFMG, at Belo Horizonte-MG) X-ray Laboratory. XRD spectra were recorded with a PANalytical X'Pert PRO diffraction instrument with theta-theta geometry, using a Cu K α X-ray source (40 kV and 45 mA). The diffraction data were collected with a step size of 0.02° 2 θ and a scan step of 0.5 s. To obtain lattice parameters of high accuracy, the diffraction data were fitted by

Rietveld methods^[41].

3.4. Whole-Rock Sm-Nd Isotopic Analyses

Sm-Nd isotopes of metamafic samples were obtained at the Isotope Geology Laboratory at Rio Grande do Sul Federal University (LGI-UFRGS). Isotopic data were acquired in static mode using a Thermo Fisher Multi-collector Mass Spectrometer Triton Plus—Thermal Ionization Mass Spectrometry (TIMS). The analytical routine included standard dissolution procedures with HCl, HNO₃, and HF in Teflon vials warmed on a hot plate to complete the material dissolution. Rare-earth elements (REE) concentration from a 1 mL aliquot was determined using column procedures with AG50W-X8 cationic resin (200–400 mesh). Posterior separation of Nd from REE was performed using anionic exchange LNB50-A resin columns (100 to 200 μm). The neodymium ratios were corrected for fractionation during normalization analysis for a $^{146}\text{Nd}/^{144}\text{Nd}$ ratio of 0.7219 and adjusted for instrumental bias based on SPEX Nd standard, assuming $^{143}\text{Nd}/^{144}\text{Nd} = 0.511110$ and calibrated against Nd for BHVO-1 standard values of $^{143}\text{Nd}/^{144}\text{Nd} = 0.512100 \pm 0.000002$. ϵNd and $^{143}\text{Nd}/^{144}\text{Nd}(t)$ were calculated for rock crystallization age. During the analysis, the Nd blank concentration was less than 160 pg. The raw data were reduced using Excel macros produced in the LGI. The initial isotope ratios of $^{143}\text{Nd}/^{144}\text{Nd}$ were calculated using the metamorphic age of 2.05 Ga obtained by Pereira and coauthors^[32]. All geochemical and isotopic calculations were performed using Geochemical Data Toolkit software^[42]. The TDM calculations were performed as described by Liew and Hofmann^[43].

4. Results

4.1. Petrography, X-Ray Diffraction, Raman Spectroscopy, and C Isotopes of Metapelites

Through observation using a petrographic microscope, it was possible to characterize the metapelites as phyllonites, that is, mylonitized metapelites. They have quartz-rich layers exhibiting polygonal grain bound-

aries that form lens-shaped pods as a result of intense shear deformation. The foliation is defined primarily by phengite and fine graphite flakes, with subordinate garnet porphyroblasts and disseminated albite microcrystals. Sample GX1 contains garnet porphyroblasts and shows the most pronounced distinction between anastomosing quartzose domains and graphite–chlorite–albite-rich layers (**Figure 4a,b**), along with distinct crenulation that overprints the main foliation. Sample GX2 contains phengite and a higher content of graphite and presents the smallest quartz grain size among the

studied samples (**Figure 4c,d**), and also hosts rotated quartz porphyroclasts with recrystallization tails. Sample MB1 shows the coarsest quartz grains within the phyllonites analyzed, a comparatively lower abundance of graphite (**Figure 4e,f**), and some plagioclase. In addition, this sample contains garnet crystals whose rims and fractures are altered to chlorite and iron oxides, as well as aggregates of fibrous cummingtonite. X-ray diffraction analyses of the phyllonites indicate a significant albite component, reaching up to 27% of the whole rock (**Figure 5**).

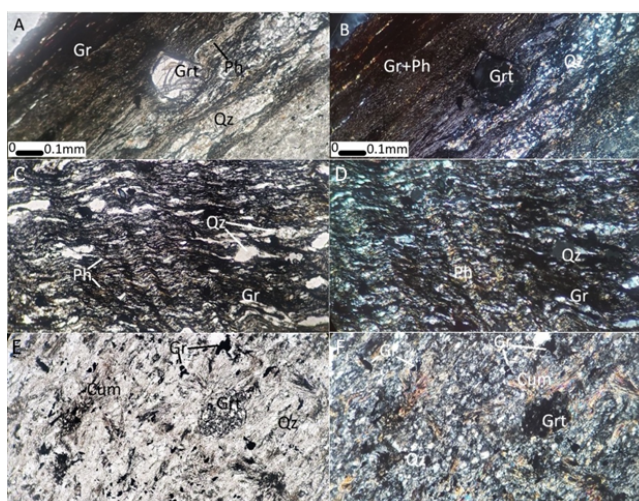


Figure 4. Phyllonites Thin-Section Images. (a) Sample GX1—Uncrossed Polarizers; (b) Sample GX1—Crossed Polarizers; (c) Sample GX2—Uncrossed Polarizers; (d) Sample GX2—Crossed Polarizers; (e) Sample MB1—Uncrossed Polarizers; (f) Sample MB1—Crossed Polarizers.

Note: Mineral abbreviations according to Whitney and Evans^[44]. Gr: graphite, Grt: garnet, Ph: phengite, Qz: quartz, Cum: cummingtonite.

The exceedingly fine-grained size of these plagioclases makes the optical identification in thin section difficult. Through Raman spectroscopy, it was possible to characterize the small albite crystals in sample GX1 along with graphite and almandine garnet; their characteristic spectra are shown in **Figure 6e,f,c,b**, respectively. Carbon isotope ($\delta^{13}\text{C}$) values, as shown in **Table 1**, range from -26.55 to -14.06 ‰, suggesting a microbial organic origin for the carbon present in the analyzed graphite populations.

4.2. Petrography, X-Ray Diffraction, and Sm-Nd Depleted Mantle Model Ages of Metamafic Rocks

The metamafic rocks are tremolite–actinolite schists comprising tremolite–actinolite, chlorite, and rare

opaque minerals. Sample MB2 shows compositional and textural banding defined by the alternation of coarse-grained and fine-grained layers (**Figure 7a,b**). The coarse-grained domains consist predominantly of actinolite, whereas the fine-grained bands comprise fibrous actinolite, chlorite, and opaque minerals. Sample MU3 shows a more homogeneous and equigranular texture, being composed mainly of tremolite, with the presence of anastomosing chlorite aggregates and disseminated albite. X-ray diffraction analyses enable the identification of the amphibole species in each sample, confirming actinolite as the predominant amphibole in MB2 and tremolite in MU3 (**Figure 8a,b**). The mineralogical assemblage of the samples suggests that the protolith of these rocks has a mafic igneous composition^[45].

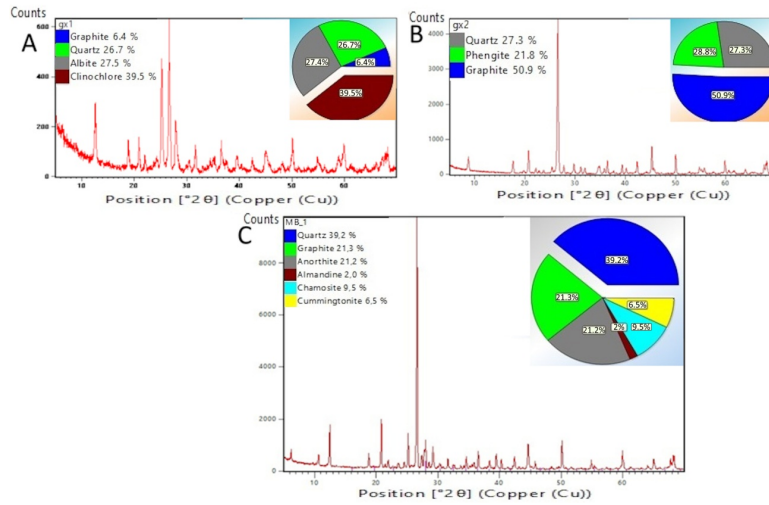


Figure 5. X-Ray Diffractograms of the Phyllonites. (a) Sample GX1; (b) Sample GX2; (c) Sample MB1.

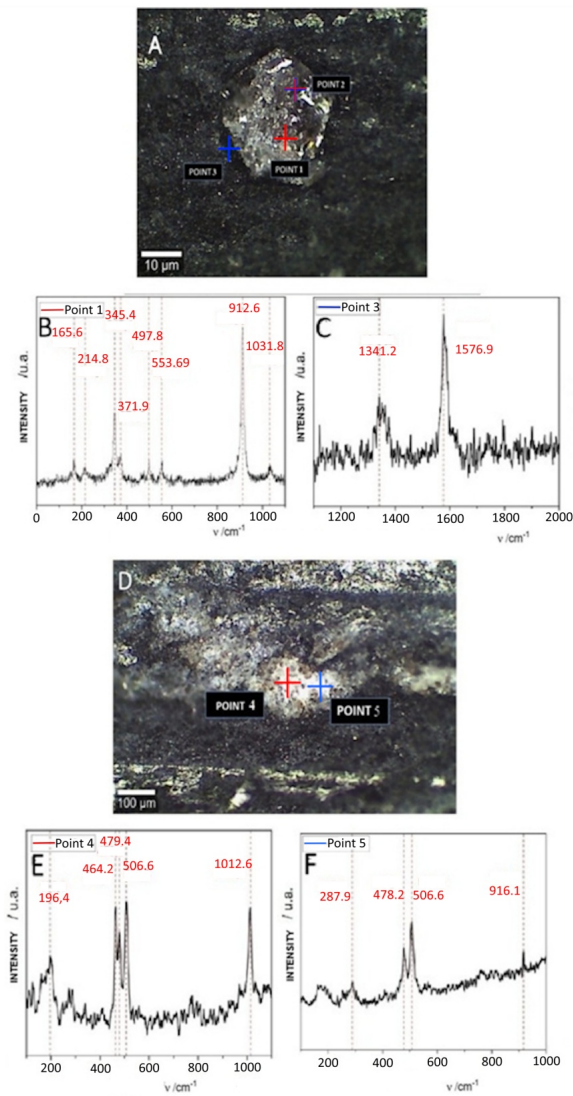


Figure 6. (a) Reflected Light Optical Images of Points 1–3; (b) Almandine, Point 1—The Point 2 is the Same Spectrum of the Point 1; (c) Graphite, Point 3; (d) Reflected Light Optical Images of Points 4 and 5; (e) Albite, Point 4 of the Sample GX1; (f) Albite, Point 5 of the Sample GX1.

Table 1. Carbon Isotopes Analysis Results.

Sample	Sample Type	$\delta^{13}\text{C} \text{ ‰ (V-PDB)}$	C%
GX1	Graphite	-26.55	2.44
GX2	Graphite	-14.06	3.15

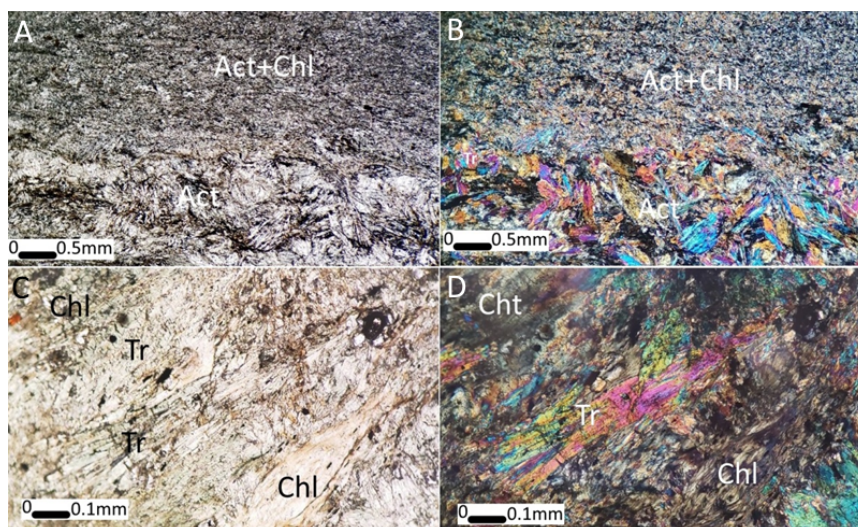


Figure 7. Thin-section images of metamafic rocks. (a) Sample MB2—Uncrossed Polarizers; (b) Sample MB2—Crossed Polarizers; (c) Sample MU3—Uncrossed Polarizers; (d) Sample MU3—Crossed Polarizers.

Note: Mineral abbreviations according to Whitney and Evans^[46]; Act: actinolite, Chl: chlorite, Tr: tremolite.

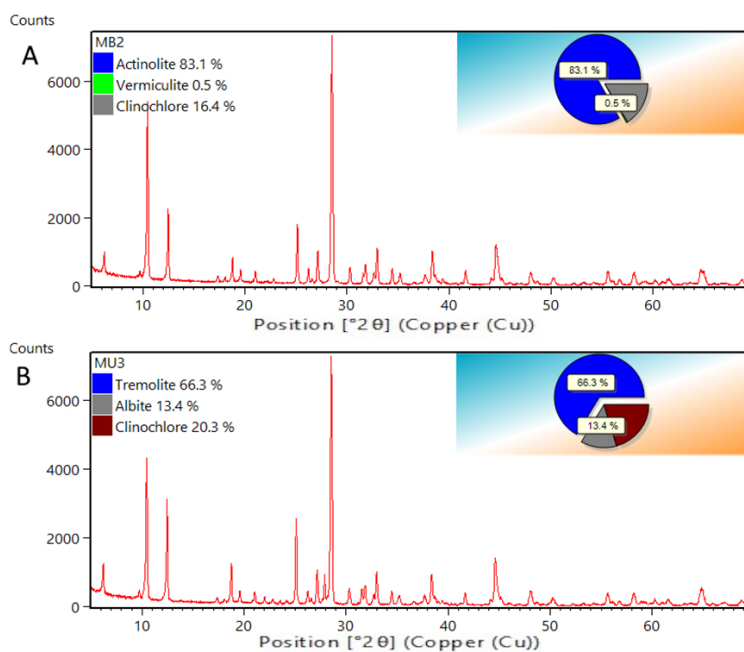


Figure 8. X-Ray Diffractograms of (a) Sample MB2; (b) Sample MU3.

Nd model age (T_{DM}) calculations were performed using single- and two-stage models, given that the rocks studied have undergone post-magmatic processes such as metamorphism. The sample MU3 displays an initial Nd isotope ratio of 0.510020 and a $\epsilon Nd(t)$ value of +0.56. The initial $^{143}\text{Nd}/^{144}\text{Nd}$ ratios for the MB2 sample are

0.510171, with calculated $\epsilon Nd(t)$ values of +3.53. The positive $\epsilon Nd(t)$ values indicate a mantle origin for the metamafic rocks. The single- and two-stage Nd model ages calculated for the MU3 are 2,354 and 2,329 Ma, respectively, while the MB2 sample shows values of 2,110 and 2,098 Ma, respectively (**Table 2**).

Table 2. Sm-Nd Isotopes Results.

Sample Name	Sm (ppm)	Nd (ppm)	$^{147}\text{Sm}/^{144}\text{Nd}$	Error (%)	$^{143}\text{Nd}/^{144}\text{Nd}$	t (Meta-Morphic Age—Ma)	ϵNd (t)	$^{143}\text{Nd}/^{144}\text{Nd}$ (t)	T_{DM} (Single Stage—Ma)	T_{DM} (Two-Stage—Ma)
MU-3	1.6510	7.7847	0.128224	0.078735	0.511746	2,050	0.56	0.510020	2,354	2,329
MB-2	4.0029	17.2880	0.139988	0.072118	0.512056	2,050	3.53	0.510171	2,110	2,098

5. Discussions

The conspicuous contrast observed in the geophysical signature (**Figure 1**) of the lithotypes proved to be an important criterion for paleoproterozoic and archean lithologic discrimination within the study area. The depleted mantle model ages (T_{DM}) obtained in this study indicate that the tremolite–actinolite schists are of Paleoproterozoic age, demonstrating that the Itatiaiuçu region can not be considered as pertaining to the Archean Rio das Velhas Supergroup as previously supposed.

The lithological association identified, comprising metaconglomerates with strongly stretched clasts and phyllonites with quartz, graphite, plagioclase, chlorite, phengite, amphibole, and garnet, is consistent with metamorphism of a structurally overprinted deep-water to syn-orogenic sedimentary sequence compatible with a convergent plate margin setting, possibly a flysch–molasse-type mélangé developed within

an accretionary orogen-related forearc basin during subduction-related shear process. Similarities between the paleoproterozoic geological setting of Itatiaiuçu and several localities where recent subduction was prevalent can be found in the scientific literature^[7–11]. The subduction tectonic context follows an evolutionary model analogous to that illustrated in **Figure 9**^[45]. The existing data (positive ϵNd values +0.56 and +3.53) corroborate a paleoproterozoic mantle source for the protolith of the tremolite-actinolite schists. Thus, tremolite-actinolite schists are interpreted as representative of metamorphosed oceanic crust, corresponding to an ocean floor that once separated the Campo Belo-Bonfim block from the Belo Horizonte and Divinópolis block at approximately 2.3 Ga ago. The transition from oceanic basin to forearc basin in a subduction context was accompanied by deformation in the folding and faulting zone, where sedimentary sequences were metamorphosed, generating metapelites (phyllonites) and metaconglomerates.

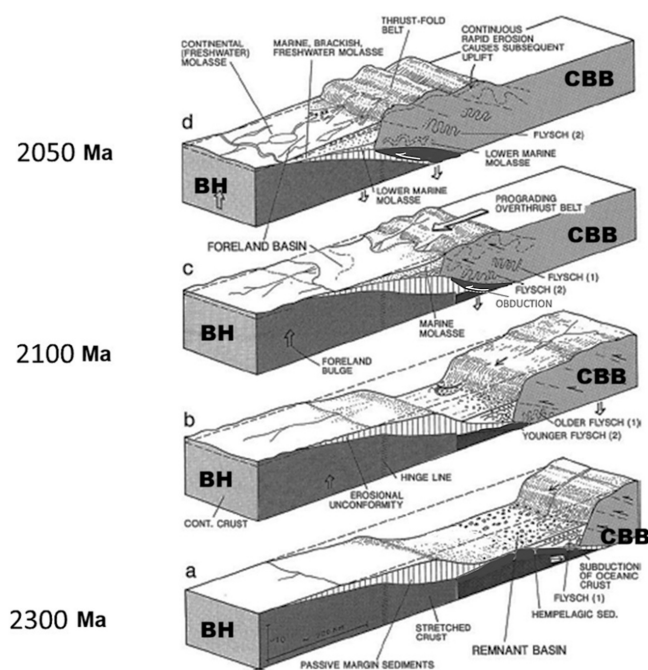


Figure 9. Schematic model (not to scale) of the transition from oceanic basin (a,b) to forearc basin (c,d) in a subduction context accompanied by deformation in the thrust belt, where flysch-molasse-type sequences are metamorphosed to generate metapelites and metaconglomerates.

Note: Remnants of obducted oceanic crust are also preserved in this model. BH—Belo Horizonte block, CBB—Campo Belo-Bonfim block. Source: Modified from Einsele^[45].

6. Conclusions

Paleoproterozoic subduction records have been recognized in nearby regions, including the identification of an accretionary prism, retro-eclogites, and retro-blueschists in the Itaguara Sequence (IS) [12,13,40], as well as the occurrence of Paleoproterozoic ophiolitic remnants not only in the IS but also in the Cláudio and Itapecerica areas [33,39,46].

In this context, the dataset obtained in this study suggests that the region located west of the Quadrilátero Ferrífero represents a tectonically significant domain that preserves multiple remnants of Paleoproterozoic geodynamic regimes comparable to those operating in modern convergent plate tectonic settings.

Author Contributions

Conceptualization, R.M.C. and A.d.O.C.; methodology, A.d.O.C. and C.C.P.; formal analysis, A.d.O.C.; investigation, R.M.C. and R.M.P.P.; resources, R.M.P.P.; writing—original draft preparation, R.M.C.; writing—review and editing, R.M.C.; visualization, R.M.P.P.; supervision, A.d.O.C. and C.C.P.; project administration, A.d.O.C. and R.M.P.P. All authors have read and agreed to the published version of the manuscript.

Funding

This work received no external funding.

Institutional Review Board Statement

Not applicable.

Informed Consent Statement

Not applicable.

Data Availability Statement

The data are available in the paper body.

Acknowledgments

The author A. Chaves thanks CNPq (Brazilian Science and Technology Agency) for the research productivity grant. Additional thanks to CPGeo-IG-USP for C isotopic analyses, CTNano/UFGM for Raman analyses, and LGI-UFRGS for Sm-Nd isotopic analyses. The authors sincerely thank the anonymous reviewers for their valuable comments and suggestions.

Conflicts of Interest

The authors declare no conflict of interest.

References

- [1] Bahlburg, H., Vervoort, J.D., Du Frane, S.A., et al., 2009. Timing of crust formation and recycling in accretionary orogens: Insights learned from the western margin of South America. *Earth-Science Reviews*. 97(1–4), 215–241. DOI: <https://doi.org/10.1016/j.earscirev.2009.10.006>
- [2] Sepidbar, F., Ao, S., Palin, R.M., et al., 2019. Origin, age and petrogenesis of barren (low-grade) granulites from the Bezenjan-Bardsir magmatic complex, southeast of the Urumieh-Dokhtar magmatic belt, Iran. *Ore Geology Reviews*. 104, 132–147. DOI: <https://doi.org/10.1016/j.oregeorev.2018.10.008>
- [3] Thakur, V.C., Misra, D.K., 1984. Tectonic framework of the Indus and Shyok suture zones in Eastern Ladakh, Northwest Himalaya. *Tectonophysics*. 101(3–4), 207–220. DOI: [https://doi.org/10.1016/0040-1951\(84\)90114-8](https://doi.org/10.1016/0040-1951(84)90114-8)
- [4] Robertson, A.H.F., 2000. Formation of mélanges in the Indus Suture Zone, Ladakh Himalaya by successive subduction-related, collisional and post-collisional processes during Late Mesozoic-Late Tertiary time. *Geological Society, London, Special Publications*. 170(1), 333–374. DOI: <https://doi.org/10.1144/GSL.SP.2000.170.01.19>
- [5] Palin, R.M., Searle, M.P., St-Onge, M.R., et al., 2015. Two-stage cooling history of pelitic and semi-pelitic mylonite (sensu lato) from the Dongjiu-Milin shear zone, northwest flank of the eastern Himalayan syntaxis. *Gondwana Research*. 28(2), 509–530. DOI: <https://doi.org/10.1016/j.gr.2014.07.009>
- [6] Parsons, A.J., Hosseini, K., Palin, R.M., et al., 2020. Geological, geophysical and plate kinematic constraints for models of the India-Asia collision and the post-Triassic central Tethys oceans. *Earth-Science Reviews*. 208, 103084. DOI: <https://doi.org/10.1016/j.earscirev.2020.103084>

- g/10.1016/j.earscirev.2020.103084
- [7] De Jong, K., 2003. Very fast exhumation of high-pressure metamorphic rocks with excess ^{40}Ar and inherited ^{87}Sr , Betic Cordilleras, southern Spain. *Lithos.* 70(3–4), 91–110. DOI: [https://doi.org/10.1016/S0024-4937\(03\)00094-X](https://doi.org/10.1016/S0024-4937(03)00094-X)
- [8] Bröcker, M., Bieling, D., Hacker, B., et al., 2004. High-Si phengite records the time of greenschist facies overprinting: implications for models suggesting mega-detachments in the Aegean Sea. *Journal of Metamorphic Geology.* 22(5), 427–442. DOI: <https://doi.org/10.1111/j.1525-1314.2004.00524.x>
- [9] Dowe, D.S., Nance, R.D., Keppie, J.D., et al., 2005. Deformational History of the Granjeno Schist, Ciudad Victoria, Mexico: Constraints on the Closure of the Rheic Ocean? *International Geology Review.* 47(9), 920–937. DOI: <https://doi.org/10.2747/0020-6814.47.9.920>
- [10] Hervé Allamand, F.E.I., Calderón, M., Faúndez, V., 2008. The metamorphic complexes of the Patagonian and Fuegian Andes. *Geologica Acta.* 43–53. DOI: <https://doi.org/10.1344/105.000000240>
- [11] Ukar, E., Cloos, M., 2016. Graphite-schist blocks in the Franciscan Mélange, San Simeon, California: Evidence of high- P metamorphism. *Journal of Metamorphic Geology.* 34(3), 191–208. DOI: <https://doi.org/10.1111/jmg.12174>
- [12] De Oliveira Chaves, A., Alexandre Goulart, L.E., Coelho, R.M., et al., 2019. High-pressure eclogite facies metamorphism and decompression melting recorded in paleoproterozoic accretionary wedge adjacent to probable ophiolite from Itaguara (southern São Francisco Craton - Brazil). *Journal of South American Earth Sciences.* 94, 102226. DOI: <https://doi.org/10.1016/j.jsames.2019.102226>
- [13] De Oliveira Chaves, A., Porcher, C.C., 2020. Petrology, geochemistry and Sm-Nd systematics of the Paleoproterozoic Itaguara retroeclogite from São Francisco/Congo Craton: One of the oldest records of the modern-style plate tectonics. *Gondwana Research.* 87, 224–237. DOI: <https://doi.org/10.1016/j.gr.2020.06.014>
- [14] CPRM—Brazilian Geological Survey, CODEMIG—Economic Development Company of Minas Gerais, 2014. Geological Map of the State of Minas Gerais. Scale 1:1,000,000 DVD-rom. CPRM, CODEMIG: Belo Horizonte, Brazil. (in Portuguese)
- [15] Teixeira, W., Ávila, C.A., Dussin, I.A., et al., 2015. A juvenile accretion episode (2.35–2.32Ga) in the Mineiro belt and its role to the Minas accretionary orogeny: Zircon U–Pb–Hf and geochemical evidences. *Precambrian Research.* 256, 148–169. DOI: <https://doi.org/10.1016/j.precamres.2014.11.009>
- [16] Baltazar, O.F., Zucchetti, M., 2007. Lithofacies associations and structural evolution of the Archean Rio das Velhas greenstone belt, Quadrilátero Ferrífero, Brazil: A review of the setting of gold deposits. *Ore Geology Reviews.* 32(3–4), 471–499. DOI: <https://doi.org/10.1016/j.oregeorev.2005.03.021>
- [17] Machado, N., Schrank, A., Noce, C.M., et al., 1996. Ages of detrital zircon from Archean–Paleoproterozoic sequences: Implications for Greenstone Belt setting and evolution of a Transamazonian foreland basin in Quadrilátero Ferrífero, southeast Brazil. *Earth and Planetary Science Letters.* 141(1–4), 259–276. DOI: [https://doi.org/10.1016/0012-821X\(96\)00054-4](https://doi.org/10.1016/0012-821X(96)00054-4)
- [18] Martínez Dopico, C.I., Lana, C., Moreira, H.S., et al., 2017. U–Pb ages and Hf-isotope data of detrital zircons from the late Neoproterozoic–Paleoproterozoic Minas Basin, SE Brazil. *Precambrian Research.* 291, 143–161. DOI: <https://doi.org/10.1016/j.precamres.2017.01.026>
- [19] Machado Filho, L., Ribeiro, M.W., Gonzalez, S.R., et al., 1983. Geology. In RADAMBRAZIL Project. Ministry of Mines and Energy, Secretariat-General: Rio de Janeiro, Brazil. pp. 36–45. (in Portuguese)
- [20] Lana, C., Alkmim, F.F., Armstrong, R., et al., 2013. The ancestry and magmatic evolution of Archaean TTG rocks of the Quadrilátero Ferrífero province, southeast Brazil. *Precambrian Research.* 231, 157–173. DOI: <https://doi.org/10.1016/j.precamres.2013.03.008>
- [21] Romano, R., Lana, C., Alkmim, F.F., et al., 2013. Stabilization of the southern portion of the São Francisco craton, SE Brazil, through a long-lived period of potassic magmatism. *Precambrian Research.* 224, 143–159. DOI: <https://doi.org/10.1016/j.precamres.2012.09.002>
- [22] Farina, F., Albert, C., Martínez Dopico, C., et al., 2016. The Archean–Paleoproterozoic evolution of the Quadrilátero Ferrífero (Brasil): Current models and open questions. *Journal of South American Earth Sciences.* 68, 4–21. DOI: <https://doi.org/10.1016/j.jsames.2015.10.015>
- [23] Moreira, H., Lana, C., Nalini, H.A., 2016. The detrital zircon record of an Archaean convergent basin in the Southern São Francisco Craton, Brazil. *Precambrian Research.* 275, 84–99. DOI: <https://doi.org/10.1016/j.precamres.2015.12.015>
- [24] Ávila, C.A., Teixeira, W., Cordani, U.G., et al., 2010. Rhyacian (2.23–2.20Ga) juvenile accretion in the southern São Francisco craton, Brazil: Geochemical and isotopic evidence from the Serrinha magmatic suite, Mineiro belt. *Journal of South American Earth Sciences.* 29(2), 464–482. DOI: <https://doi.org/10.1016/j.jsames.2009.07.009>

- [25] Alkmim, F.F., Teixeira, W., 2017. The Paleoproterozoic Mineiro Belt and the Quadrilátero Ferrífero. In: Heilbron, M., Cordani, U.G., Alkmim, F.F. (Eds.). São Francisco Craton, Eastern Brazil, Regional Geology Reviews. Springer International Publishing: Cham, Switzerland. pp. 71–94. DOI: https://doi.org/10.1007/978-3-319-01715-0_5
- [26] Bruno, H., Heilbron, M., De Morisson Valeriano, C., et al., 2021. Evidence for a complex accretionary history preceding the amalgamation of Columbia: The Rhyacian Minas-Bahia Orogen, southern São Francisco Palecontinent, Brazil. *Gondwana Research*. 92, 149–171. DOI: <https://doi.org/10.1016/j.gr.2020.12.019>
- [27] Campos, J.C.S., Carneiro, M.A., 2008. Neoproterozoic and Paleoproterozoic granitoids marginal to the Jeceaba-Bom Sucesso lineament (SE border of the southern São Francisco craton): Genesis and tectonic evolution. *Journal of South American Earth Sciences*. 26(4), 463–484. DOI: <https://doi.org/10.1016/j.jsames.2008.09.002>
- [28] Oliveira, A.H., 2004. Tectonic Evolution of a Fragment of the Southern São Francisco Craton [PhD Thesis]. Federal University of Ouro Preto: Ouro Preto, Brazil. (in Portuguese)
- [29] Coelho, R.M., Chaves, A.D.O., 2019. Pressure-temperature-time path of Paleoproterozoic khondalites from Claudio shear zone (southern São Francisco craton, Brazil): Links with khondalite belt of the North China craton. *Journal of South American Earth Sciences*. 94, 102250. DOI: <https://doi.org/10.1016/j.jsames.2019.102250>
- [30] Pereira, R.M.P., Lana, C.D.C., Porcher, C.C., et al., 2025. Ophiolitic metamafic remnants of Palaeoproterozoic oceanic crust from the Cláudio shear zone, Southern São Francisco Craton (Brazil). *International Geology Review*. 67(24), 2777–2801. DOI: <https://doi.org/10.1080/00206814.2025.2563590>
- [31] Carvalho, B.B., Sawyer, E.W., Janasi, V.A., 2016. Crustal reworking in a shear zone: Transformation of metagranite to migmatite. *Journal of Metamorphic Geology*. 34(3), 237–264. DOI: <https://doi.org/10.1111/jmg.12180>
- [32] Carvalho, B.B., Janasi, V.A., Sawyer, E.W., 2017. Evidence for Paleoproterozoic anatexis and crustal reworking of Archean crust in the São Francisco Craton, Brazil: A dating and isotopic study of the Kinawa migmatite. *Precambrian Research*. 291, 98–118. DOI: <https://doi.org/10.1016/j.precamres.2017.01.019>
- [33] Teixeira, W., Oliveira, E.P., Peng, P., et al., 2017. U-Pb geochronology of the 2.0 Ga Itapeceira graphite-rich supracrustal succession in the São Francisco Craton: Tectonic matches with the North China Craton and paleogeographic inferences. *Precambrian Research*. 293, 91–111. DOI: <https://doi.org/10.1016/j.precamres.2017.02.021>
- [34] Miranda, D.A., De Oliveira Chaves, A., Campello, M.S., et al., 2019. Origin and thermometry of graphites from Itapeceira supracrustal succession of the southern São Francisco Craton by C isotopes, X-ray diffraction, and Raman spectroscopy. *International Geology Review*. 61(15), 1864–1875. DOI: <https://doi.org/10.1080/00206814.2018.1564073>
- [35] Miranda, D.A., Chaves, A.D.O., Dussin, I.A., et al., 2021. Paleoproterozoic khondalites in Brazil: a case study of metamorphism and anatexis in khondalites from Itapeceira supracrustal succession of the southern São Francisco Craton. *International Geology Review*. 63(4), 397–421. DOI: <https://doi.org/10.1080/00206814.2020.1716273>
- [36] Goulart, L.E.A., Carneiro, M.A., 2010. Paleoproterozoic mafic-ultramafic magmatism in the southern São Francisco Craton: The Itaguara layered sequence. In *Proceedings of the Brazilian Geological Congress, Belém, Brazil, 26 September–1 October 2010*. (in Portuguese)
- [37] Goulart, L.E.A., Carneiro, M.A., 2008. General characteristics and litho-geochemistry of the Itaguara layered ultramafic-mafic sequence, southern São Francisco craton. *Geochimica Brasiliensis*. 22, 45–72.
- [38] Pinheiro, S.D.O., Nilson, A.A., 2000. Metakomatiitic and Meta-Ultramafic Rocks from the Rio Manso Region, Minas Gerais: Geology Textures and Metamorphism. *Revista Brasileira de Geociências*. 30(3), 421–423.
- [39] Barbosa, A.D.S., Chaves, A.D.O., 2022. Itaguara amphibolites with E-MORB signature: Probable Paleoproterozoic ophiolite members of the southern São Francisco craton. *Geociências*. 40(4), 853–861. DOI: <https://doi.org/10.5016/geociencias.v40i04.16005> (in Portuguese)
- [40] De Oliveira Chaves, A., 2024. 2.13 Ga Lawsonite/Barroisite-Bearing E-MORB Signature Metagabbro Associated with Spinel Metaperidotite from Itaguara (São Francisco Craton, Brazil): Oldest Blueschist-Facies Fragment of Oceanic Moho? *Earth and Planetary Science*. 3(2), 14–40. DOI: <https://doi.org/10.36956/eps.v3i2.1068>
- [41] Young, R.A., 1993. *The Rietveld Method*. Oxford University Press: Oxford, UK.
- [42] Janoušek, V., Farrow, C.M., Erban, V., 2006. Interpretation of Whole-rock Geochemical Data in Igneous Geochemistry: Introducing Geochemical Data Toolkit (GCDkit). *Journal of Petrology*. 47(6), 1255–1259. DOI: <https://doi.org/10.1093/petrology/egl013>
- [43] Liew, T.C., Hofmann, A.W., 1988. *Precambrian*

- crustal components, plutonic associations, plate environment of the Hercynian Fold Belt of central Europe: Indications from a Nd and Sr isotopic study. *Contributions to Mineralogy and Petrology*. 98(2), 129–138. DOI: <https://doi.org/10.1007/BF00402106>
- [44] Whitney, D.L., Evans, B.W., 2010. Abbreviations for names of rock-forming minerals. *American Mineralogist*. 95(1), 185–187. DOI: <https://doi.org/10.2138/am.2010.3371>
- [45] Einsele, G., 2000. *Sedimentary Basins: Evolution, Facies, and Sediment Budget*, 2nd ed. Springer: London, UK.
- [46] Miranda, D.A., Chaves, A.D.O., 2021. Itapacerica Metamafic-Ultramafic Rocks with E-Morb Signature: Ophiolitic Remnants of the Rhyacian-Orosirian Orogeny in Southern São Francisco Craton? *Geociências*. 40(1), 1–12. DOI: <https://doi.org/10.5016/geociencias.v40i1.15375> (in Portuguese)